Journal of Natural Disaster Science, Volume 25, Number 2, 2003, pp93-101

Simulation of Earthquake Motion from Phase Information

Tadanobu SATO
Disaster Prevention Research Institute, Kyoto University, Uji Kyoto 611-0011, Japan
Yoshitaka MURONO
Rail Way Research Institute, Hikari-Cho, Kokubunji 185-8540, Tokyo Japan

(Received for 10. May, 2003 and in revised form 1 Dec., 2003)

ABSTRACT

We developed a method based on the concept of wavelet transformation to simulate earthquake motion that uses phase spectra of earthquake motions. By using Mayer's analyzing wavelet a simultaneous linear equation was derived from which the relative values of wavelet coefficients can be determined from the phase spectrum on each compact support of a scale function. The relationship between the power of earthquake motions and the wavelet coefficients on each compact support was used to determine the absolute values of wavelet coefficients. The efficiency of the proposed method was investigated by comparing resimulated with observed earthquake motion. A stochastic model with which to simulate the phase spectrum is proposed that is based on the concept of group delay time. A sample phase spectrum simulated by this stochastic model was used to simulate an artificial earthquake motion based on the proposed method.

1. INTRODUCTION

Estimation of the responses of structural systems based on dynamic analyses is essential for the seismic design of civil structures. How design earthquake motions should be defined has been a main concern of civil engineers since the 1995 Hyogoken Nambu earthquake in Japan (JSCE 1996).

Methods used to simulate design earthquake motion fall into three categories: (i) Theoretical methods based on the source rapture mechanism and elastic wave propagation theories, (ii) Methods using the empirical Green's function, (iii) Stochastic simulation methods. Methods in (i) and (ii) can be used to simulate precise earthquake motion at a design point if detailed information can be provided to define the fault mechanism, propagating path and local site effects. Earthquake motions that are used for establishing measures against future earthquake damage sometimes are simulated theoretically using scenario earthquakes and taking into account the seismic environment in the area of concern (Irikura 2000). But to design conventional civil structures, such as small bridges, this method is not practical because the position of the active fault and its source parameter, which control the rupture mechanism, can not be easily determined.

Methods in class (iii) often are used to define design earthquake motions because they have simple forms and only small number of parameters are needed to define the models. A primitive method developed during the early stage studies of this category was to generate a stationary time history by summing up the harmonic waves with random amplitudes and phases (Yang 1972). The nonstationary power spectrum was modeled by a regression equation as a function of earthquake magnitude and epicentral distance (Kameda 1977), and based on the results, a method to simulate nonstationary strong motion was developed (Goto et al. 1979). Most often used method simulates earthquake motion from amplitude spectra expressed by the attenuation relationship and a random phase. To guarantee nonstationarity, an envelope function is multiplied to the stationary time history simulated by means of a random phase (Jennings et al. 1968).

The modeling of amplitude spectra has claimed the attention of many researchers. The attenuation relationship of the Fourier amplitude was derived in the U.S.A. in the late 1970s (Trifunac 1976) and that of response spectra was proposed in Japan in late 1980s (Kamiyama and Ynagisawa 1986, Kawashima et al. 1984). Moreover to account for the fault extent the concept of equivalent source distance was introduced (Ohno et al. 1993). Based on the two-stage least square method (Joyner and Boore 1981) that eliminates the dependency between magnitude and distance, Fukushima (1994) derived an attenuation relationship by using shortest distance to earthquake faults. Rapture directivity also was introduced into the attenuation of response spectrum in the case of using the equivalent source distance (Ohno et al. 1998).

Several pioneer works clarified the nonstationary characteristics of earthquake motions through the analyses of their phase characteristics. Osaki et al. (1984) showed a similarity between the distribution width of the phase difference and the duration of earthquake motion. Izumi and Katsukura (1980) who used the concept of group delay time, showed that the average arrival time of earthquake energy and the duration of earthquake motion can be evaluated by the mean and standard deviation of the group delay time. Sawada et al. (1986), Ishi et al. (1987), and Satoh et al. (1996) analyzed the phase difference or the group delay time of earthquake motions and derived attenuation relationships related to the duration, mean and standard deviation of the group delay time. We also studied the phase characteristic of earthquake motions and developed two methods (Sato et al. 1999a, 1999b) to simulate phase

KEY WORDS: Phase spectra, simulation of earthquake motion, wavelet coefficient, wavelet transform, group delay time

spectra. One is the modeling of phase spectra near the source region, taking into account the source rupture mechanism, propagating path and local soil condition (Sato et al. 1999a). The other is the modeling of phase spectra using the concept of group delay time and wavelet analyses, in which we proposed regression relationships that express the mean group and the standard deviation of the group delay time as functions of epicentral distance and earthquake magnitude (Sato et al. 1999b). Using the models developed to simulate phase spectra, we simulated earthquake motions compatible with design acceleration response spectra.

The simulated motions based on these methods, however, do not satisfy causality because the amplitude and phase spectra must be given independently. The purpose of the study reported here was to overcome this deficiency in simulating design earthquake motions and to develop a simulation method compatible with given phase spectra.

2. THEORY

(1) Algorithm for Simulating Earthquake Motions Compatible with Phase Spectra

A method to simulate a time history on the scale factor of Mayer's analyzing wavelet is developed when the group delay time or phase spectrum is given on this scale factor. If the wavelet coefficients a_{jk} of the time history $f(t)$ are given, the discrete inverse wavelet transformation is defined by (Sasaki et al. 1992)

$$f(t)=\sum_{j=1}^{M}\sum_{k=0}^{N-1}a_{jk}\cdot\varphi_{jk}(t) \tag{1}$$

in which N is given by 2^j (j=1,2,⋯,M), and the total number of digitized points in time is 2^M, and $\psi_{jk}(t)$ is the analyzing wavelet defined by

$$\varphi_{jk}(t)=\varphi\left(2^jT^{-1}t-k\right) \tag{2}$$

The decomposed time history $f_j(t)$ of an earthquake motion on the jth scale factor is expressed by

$$f_j(t)=\sum_{k=0}^{N-1}a_{jk}\cdot\varphi_{jk}(t) \tag{3}$$

If we compose an analyzing wavelet by the method of Mayer (1989), this wavelet has a compact support in the frequency domain, and the Fourier transform of equation (3) is

$$F_j(\omega)=\sum_{k=0}^{N-1}a_{jk}\cdot T^{1/2}\cdot 2^{-j/2}\cdot e^{-i\omega\frac{Tk}{2^j}}\cdot\Psi\left(2^{-j}T\omega\right) \tag{4}$$

in which T is the duration of earthquake motion and $\Psi(\omega)$ the Fourier transform of the analyzing wavelet $\psi(t)$ expressed by

$$\Psi(\omega)=\int_{-\infty}^{\infty}\varphi(t)\cdot e^{-i\omega t}dt \tag{5}$$

Furthermore, we can rewrite equation (4):

$$F_j(\omega)=A_j(\omega)e^{-\phi_j(\omega)}=\Psi_j(\omega)\sum_{k=0}^{N-1}a_{jk}\cdot e^{-i\omega t_{jk}} \tag{6}$$

in which $A_j(\omega)$ and $\phi_j(\omega)$ respectively are the amplitude and phase spectra of $F_j(\omega)$. The values of t_{jk} and $\Psi_j(\omega)$ have the following form when Meyer's formulation of the analyzing wavelet (Mayer 1989) is used;

$$t_{jk}=\frac{Tk}{2^j} \tag{7}$$

$$\begin{aligned}\Psi_j(\omega)&=T^{1/2}2^{-j/2}\Psi\left(2^{-j}T\omega\right)\\&=T^{1/2}2^{-j/2}\cdot exp\left(-i\omega 2^{-j-1}T\right)\\&\quad\cdot\sqrt{\left(\Phi\left(2^{-j-1}T\omega\right)\right)^2+\left(\Phi\left(2^{-j}T\omega\right)\right)^2}\end{aligned} \tag{8}$$

where $\Phi(\omega)$ is a scaling function. If the amplitude and phase spectra of the summation term in equation (6) are expressed by $A_j^p(\omega)$ and $\phi_j^p(\omega)$ then

$$A_j^p(\omega)e^{-i\phi_j^p(\omega)}=\sum_{k=0}^{N-1}a_{jk}e^{-i\omega t_{jk}} \tag{9}$$

in which $A_j^p(\omega)$ and $\phi_j^p(\omega)$ are defined by

$$A_j^p(\omega)=\sqrt{\left\{\sum_{k=0}^{N-1}a_{jk}\,sin\left(\omega t_{jk}\right)\right\}^2+\left\{\sum_{k=0}^{N-1}a_{jk}\,cos\left(\omega t_{jk}\right)\right\}^2} \tag{10}$$

$$\phi^p(\omega)=tan^{-1}\left\{-\frac{\sum_{k=0}^{N-1}a_{jk}\,sin\left(\omega t_{jk}\right)}{\sum_{k=0}^{N-1}a_{jk}\,cos\left(\omega t_{jk}\right)}\right\} \tag{11}$$

The relationship between $\phi_j(\omega)$ and $\phi^p(\omega)$ is obtained from equations (6), (8) and (11)

$$\phi_j(\omega)=\phi_j^p(\omega)-\omega\left(\frac{T}{2^{j+1}}\right) \tag{12}$$

If the value of $\phi_j(\omega)$ is given, the following equation is obtained by substituting equation (11) into equation (12)

$$\sum_{k=0}^{N-1}\left\{cos\left(\omega t_{jk}\right)\cdot\beta_j(\omega)+sin\left(\omega t_{jk}\right)\right\}\cdot a_{jk}=0 \tag{13}$$

in which

$$\beta_j(\omega)=tan\left(\phi_j(\omega)+\omega T/2^{j+1}\right) \tag{14}$$

To solve equation (13) with respect to a_{jk}, we consider m discrete circular frequency points (i=1,2,⋯,m) on the compact support of the jth scale factor and define a new variable

$$\alpha_{jk}(\omega_i)=\beta_j(\omega_i)\cdot cos\left(\omega_i t_{jk}\right)+sin\left(\omega_i t_{jk}\right) \tag{15}$$

k=0,1,⋯, 2^j-1, i=1,2,⋯,m

Equation (14) is then rewritten

$$\begin{bmatrix} \alpha_{j0}(\omega_1) & \alpha_{j1}(\omega_1) & \cdots & \alpha_{jN-1}(\omega_1) \\ \alpha_{j0}(\omega_2) & \alpha_{j1}(\omega_2) & & \alpha_{jN-1}(\omega_2) \\ \vdots & & \ddots & \vdots \\ \alpha_{j0}(\omega_m) & \alpha_{j1}(\omega_m) & \cdots & \alpha_{jN-1}(\omega_m) \end{bmatrix} \begin{Bmatrix} a_{j0} \\ a_{j1} \\ \vdots \\ a_{jN-1} \end{Bmatrix} = \begin{Bmatrix} 0 \\ 0 \\ \vdots \\ 0 \end{Bmatrix} \tag{16}$$

Because equation (16) is a homogeneous simultaneous equation, we assume the condition a_{j0}=1 to obtain the ratio of a_{jk} to a_{j0}, as expressed by $\bar{a}_{jk}$ (k=1,2,⋯,N-1)

$$\begin{bmatrix} \alpha_{j1}(\omega_1) & \alpha_{j2}(\omega_1) & \cdots & \alpha_{jN-1}(\omega_1) \\ \alpha_{j1}(\omega_2) & \alpha_{j2}(\omega_2) & & \alpha_{jN-1}(\omega_2) \\ \vdots & & \ddots & \vdots \\ \alpha_{j1}(\omega_m) & \alpha_{j2}(\omega_m) & \cdots & \alpha_{jN-1}(\omega_m) \end{bmatrix} \begin{Bmatrix} \bar{a}_{j1} \\ \bar{a}_{j2} \\ \vdots \\ \bar{a}_{jN-1} \end{Bmatrix} = -\begin{Bmatrix} \alpha_{j0}(\omega_1) \\ \alpha_{j0}(\omega_2) \\ \vdots \\ \alpha_{j0}(\omega_m) \end{Bmatrix} \tag{17}$$

For simplicity equation (17) is rewritten

$$[A]\cdot\{\bar{a}_{jk}\} = -\{B\} \tag{18}$$

in which the dimension of matrix [A] is $m\times(N\text{-}1)$. The number of unknowns is N-1 but the order of equation (18) is m. The least squares method is used to obtain $\bar{a}_{jk}$ by means of the QR deconvolution technique of matrix [A].

To determine the absolute value of a_{jk}, a relation is required to define the value of a_{j0}. We assume that the power of earthquake motion is exerted on the compact support of jth scale factor. Perseval's equality gives

$$\int_{-\infty}^{\infty} |f_j(t)|^2 dt = \frac{1}{2\pi}\int_{-\infty}^{\infty} |F_j(\omega)|^2 d\omega \tag{19}$$

Using equation (3), the left hand side integral is expressed by

$$\int_{-\infty}^{\infty} |f_j(t)|^2 dt = \int_{-\infty}^{\infty}\left(\sum_{k=0}^{N-1} a_{jk}\varphi_{jk}(t)\right)^2 dt \tag{20}$$

Taking into account the fact that Mayer's analyzing wavelet comprises a completely orthonormal system;

$$\int_{-\infty}^{\infty} |f_j(t)|^2 dt = \sum_{k=0}^{N-1} a_{jk}^2\left(\frac{1}{2\pi}\int_{-\infty}^{\infty} |\Psi_j(\omega)|^2 d\omega\right) \tag{21}$$

Combining equations (19) and (21) and taking into account $a_{jk} = a_{j0}\cdot\bar{a}_{jk}$, the equation (19) becomes

$$\int_{-\infty}^{\infty} |F_j(\omega)|^2 d\omega = a_{j0}^2\cdot\left(1.0+\sum_{k=1}^{N-1}\bar{a}_{jk}^2\right)\cdot\int_{-\infty}^{\infty}|\Psi_j(\omega)|^2 d\omega \tag{22}$$

If Mayer's analyzing wavelet is used, the integral appearing on the right side of equation (22) is

$$\int_{-\infty}^{\infty} |\Psi_j(\omega)|^2 d\omega = 2\pi \tag{23}$$

The left side of equation (22) is equal to the power of the earthquake motion on the compact support of jth scale factor. We assume that this is expressed by λ_j^2 as

$$\lambda_j^2 = \int_{-\infty}^{\infty} |F_j(\omega)|^2 d\omega \tag{24}$$

Substituting equations (23) and (24) into equation (22) gives the expression for a_{j0};

$$\begin{aligned} a_{j0} &= \lambda_j \Big/ \sqrt{2\pi\left(1.0+\sum_{k=1}^{n-1}\bar{a}_{jk}^2\right)} \\ &= \lambda_j \Big/ \sqrt{2\pi\sum_{k=0}^{n-1}\bar{a}_{jk}^2} \end{aligned} \tag{25}$$

Once a_{j0} is given, the value of a_{jk} compatible with the phase spectrum $\phi_j(\omega)$ is determined, after which the decomposed time history of earthquake motion on the jth scale factor $f_j(t)$ can be resimulated.

(2) Algorithm for Simulating Earthquake Motion Compatible with the Amplitude Spectrum

The wavelet coefficients can be determined by using the amplitude spectrum of earthquake motion. If the amplitude spectrum of the time history on the jth scale factor $A_j(\omega)$ is given the following equation is obtained from equation (6)

$$A_j(\omega) = A_j^p(\omega)\cdot|\Psi_j(\omega)| \tag{26}$$

in which $A_j^p(\omega)$ is defined in equation (10). Substituting equation (10) into equation (26) gives

$$\begin{aligned} A_j^2(\omega) = \sum_{k=0}^{N-1} a_{jk}^2 |\Psi_j(\omega)|^2 + 2\sum_{k=0}^{N-1}\sum_{l=k+1}^{N-1} a_{jk}|\Psi_j(\omega)|\cdot \\ a_{jl}|\Psi_j(\omega)|\cdot cos\{\omega(t_{jl}-t_{jk})\} \end{aligned} \tag{27}$$

Because this is a nonlinear equation with respect to ajk, it is not so easy to construct an algorithm to obtain ajk. In the following analyses a method to determine an a_{jk} compatible with the phase spectrum therefore was used.

3. VERIFICATION OF THE METHOD DEVELOPED

This was made using the observe ground motion at Morioka during the 1994 Off Sanriku earthquake. Fig.1 shows the wavelet coefficients, a_{jk}, on the scale factor of j=5～12, and Fig.2 the decomposed time history $f_j(t)$ on each scale factor. The Fourier amplitude spectrum is shown in Fig.3. The frequency range of Meyer's analyzing wavelet on the compact support of the jth scale factor is

$$\left\{f \mid 2^j/3T \le f \le 2^{j+2}/3T\right\} \tag{28}$$

in which T is the duration of earthquake motion. Each support is overlapped by neighboring supports (Fig.3). The central frequancy range of each support (Sato et al. 1999b) is

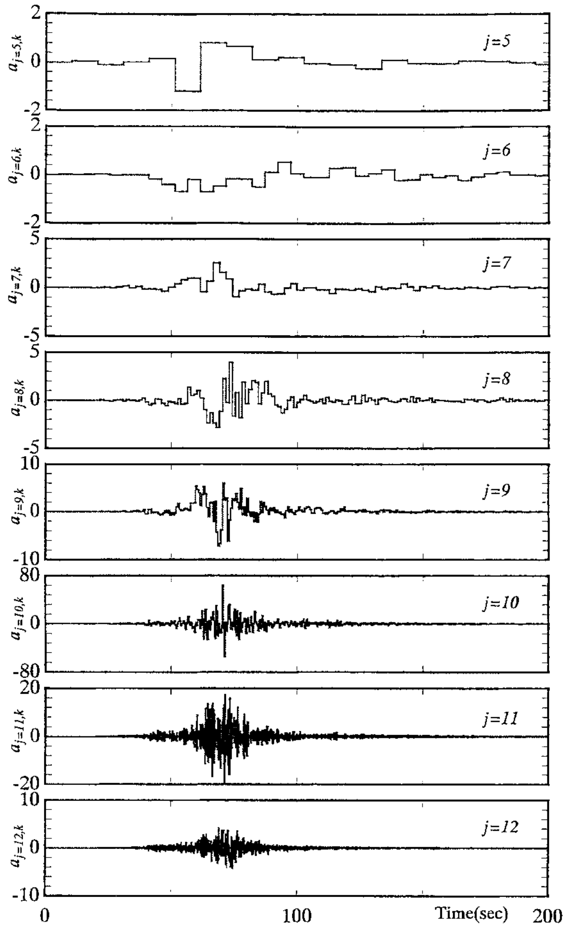

Fig. 1 Wavelet coefficients for each scale factor j (j=5～12)

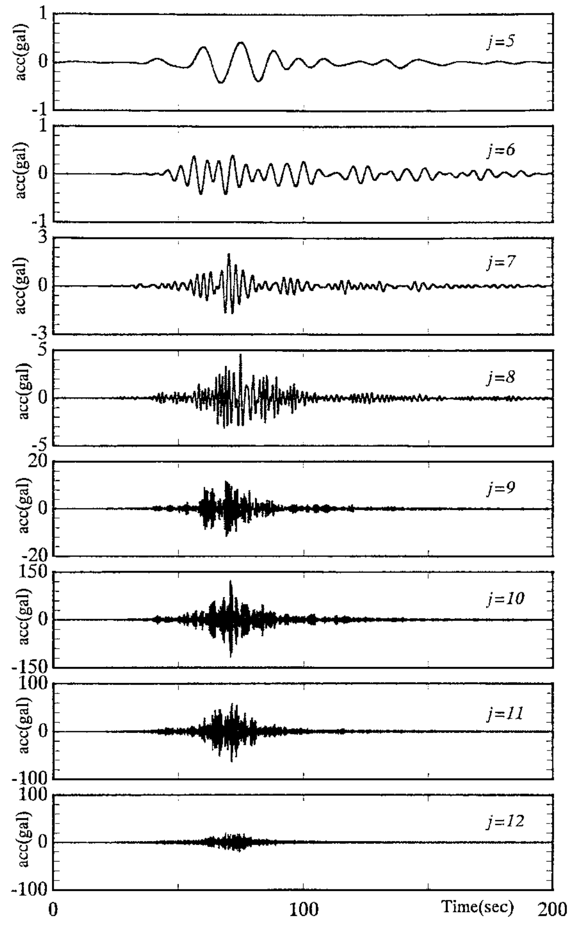

Fig. 2 Wavelet decomposed wave for each scale factor j (j=5～12)

$$\left\{f \mid 2^{j-1}/T \le f \le 2^{j}/T\right\} \tag{29}$$

shown by broken lines in Fig.3.

To determine the a_{jk} wavelet coefficients as being able to express precisely the phase spectrum for the frequency range defined by equation (29) we selected m discrete circular frequencies, ω_i (i=1, 2,⋯, m), in this frequency range and calculated $\phi_j(\omega_i)$ after which we detemine the a_{jk} wavelet coefficients using equations (17) and (25).

For the case of j=5 Figs.4 and 5 show the time history of wavelet coefficients a_{5k} and the recomposed time history $f_{j=5}(t)$. Three m values (32, 64, 128) were considered to determine the effect of number of discrete points, m, on the identified wavelet coefficients. The case of m=32 is equivalent to $2^{j\,(j=5)}$, and is one value larger than the number of unkown values $\overline{a}_{jk}$ (k=1,…,31). As the number of discrete points increases, the duration of the composed time signal increases. We therefore used $m=2^j$ for the following caluculations.

For the case of j=5～12 the time history of the a_{jk} wavelet coefficients are shown in Figs.6 and the recomposed time history $f_j(t)$ in Fig.7. A comparison of Figs. 2 and 3 shows that the recomposed time histories agree well with the decomposed time histories from the observed earthquake motion for all the j values. Resimulated earthquake motion summing up the recomposed time history for j=5～12 is shown in Fig.8. Nonlinear response spectra

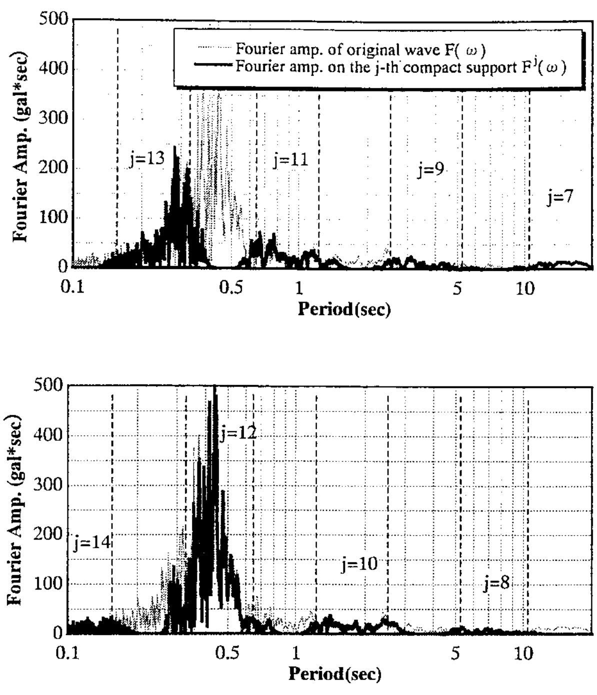

Fig. 3 Fourier amplitude of the wavelet decomposed wave for each compact support

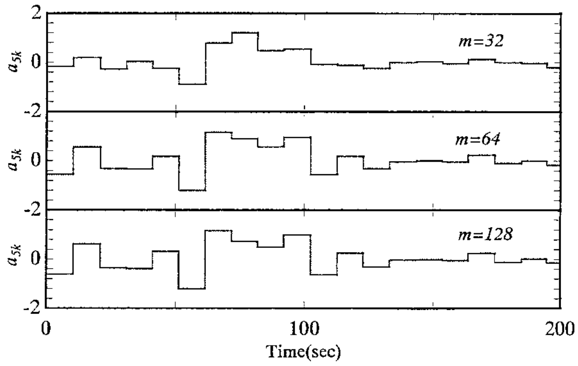

Fig. 4 Simulated wavelet coefficients for j=5

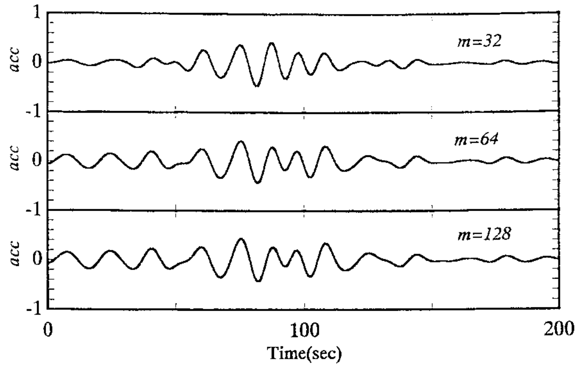

Fig. 5 Simulated decomposed wavelet for j=5

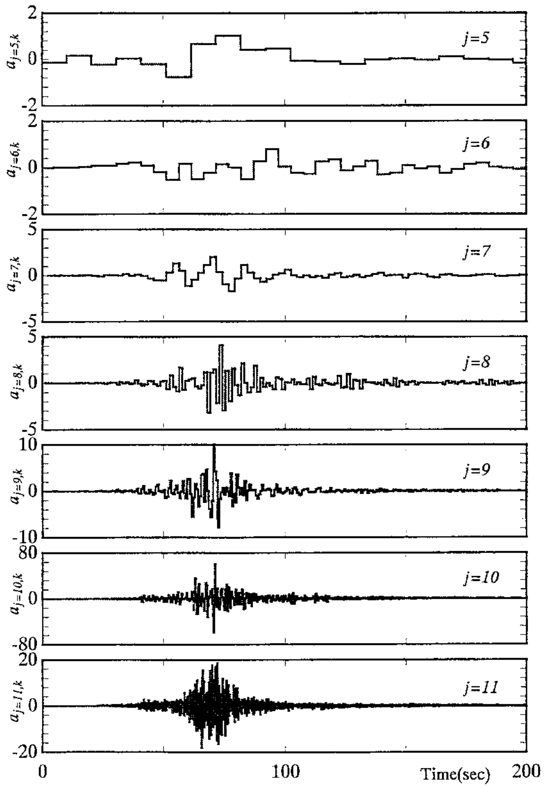

Fig. 6 Simulated wavelet coefficients for each scale factor j (j=5～11)

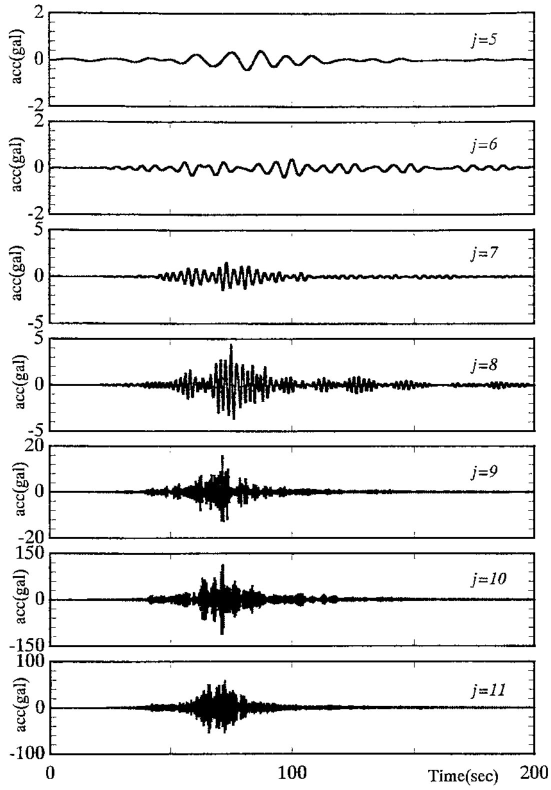

Fig. 7 Simulated decomposed waves for the scale j (j=5～11)

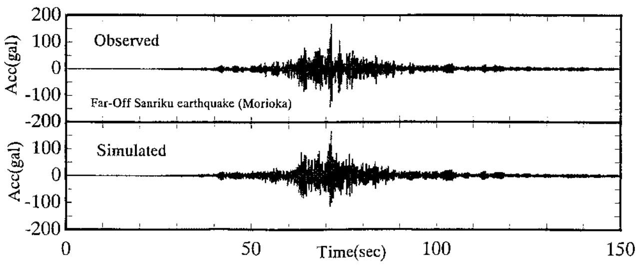

Fig. 8 Comparison of observed and simulated seismograms

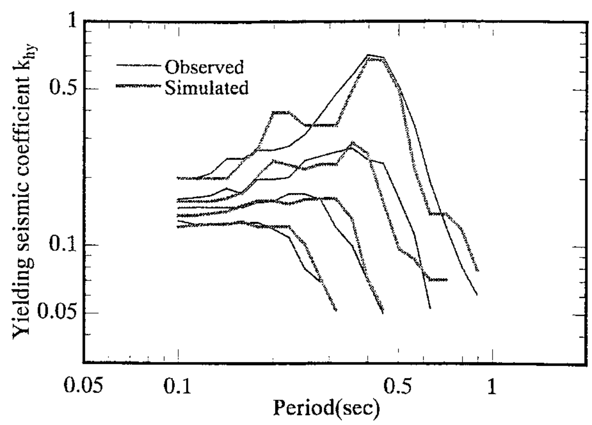

Fig. 9 Comparison of non-linear response spectra calculated from observed and simulated seismograms

(ductility demand spectra) calculated with this resimulated earthquake motion are shown in Fig.9. For comparison those calculated using the band-passed (correspond to the frequency range j=5~12) observed earthquake motion also are shown. Not only wave forms, but the nonlinear response characteristics of the structural system obtained using resimulated earthquake motion agree well with those of the observed earthquake motion.

4. MODELING PHASE SPECRA USING GROUP DELAY TIME

We developed a simple model to simulate phase spectra using the concept of group delay time and wavelet analysis. The group delay time of each earthquake motion was calculated on each compact support of Mayer's analyzing wavelet using existing data sets of observed earthquake motions. If the phase spectrum of a time history of the jth scale $\phi^{(j)}(\omega)$ is given, the group delay time on the jth compact support at the circular frequency of ω_i is defined by

$$t_{gr}^{(j)} = \frac{d\phi^{(j)}}{d\omega} = -\frac{\phi^{(j)}(\omega_i) - \phi^{(j)}(\omega_{i+1})}{\Delta\omega} \tag{30}$$

Because of the fluctuating nature of the group delay time on each compact support the mean value of the group delay time, $\sigma_{tgr}^{j}(\omega)$, and standard deviation, $\sigma_{tgr}^{j}(\omega)$, were calculated;

$$\mu_{tgr}^{(j)} = \sum_{i=1}^{N^{(j)}} \frac{t_{gr}^{(j)}(\omega_i)}{N^{(j)}} \qquad \sigma_{tgr}^{(j)} = \sqrt{\frac{1}{N^{(j)}}\sum_{i=1}^{N^{(j)}}\left(t_{gr}^{(j)}(\omega_i) - \mu_{tgr}^{(j)}\right)^2} \tag{31}$$

Regression equations as functions of epicentral distance, Δ, and the earthquake magnitudes, M, for these values were derived (Sato et al. 1999b).

$$\mu_{tgr}^{(j)} = \alpha_1^{(j)} \times 10^{\beta_1^{(j)}M} \times \Delta^{\gamma_1^{(j)}} \tag{32}$$

$$\sigma_{tgr}^{(j)} = \alpha_2^{(j)} \times 10^{\beta_2^{(j)}M} \times \Delta^{\gamma_2^{(j)}} \tag{33}$$

The power on the jth support, λ_j^2, also is expressed by the regression equation

$$\lambda_j^2 = \alpha_3^{(j)} \times 10^{\beta_3^{(j)}M} \times \Delta^{\gamma_3^{(j)}} \tag{34}$$

The observed earthquake motion data sets used are from the 1993 Off South West Hokkaido earthquake (M7.8), the 1994 Off East Hokkaido earthquake (M8.1), the 1995 Far-off Sanriku earthquake (M7.5), the 1995 Hyogoken Nambu earthquake (M7.2) and the 1997 East Kagoshimaken earthquake (M6.3).

Results of the regression analyses are shown in Table 1 and Fig.10. Except for j=7, the value of λ_j^2 increases as M increases and attenuates with the epicentral distance. The effect of M and Δ on the value of λ_j^2 becomes less remarkable for small j values. The value of λ_j^2 is not solely affected by earthquake magnitude and epicentral distance, but by soil conditions of the site as well. Classifying the value of $\alpha_3^{(j)}$ from the soil or site classification (Kamiyama and Yanagisawa 1986, Kawashima et al. 1984) improves the accuracy of the regression equation, but for simplicity those effects are neglected. The saturation effect of attenuation relationship at the near source region is also not considered.

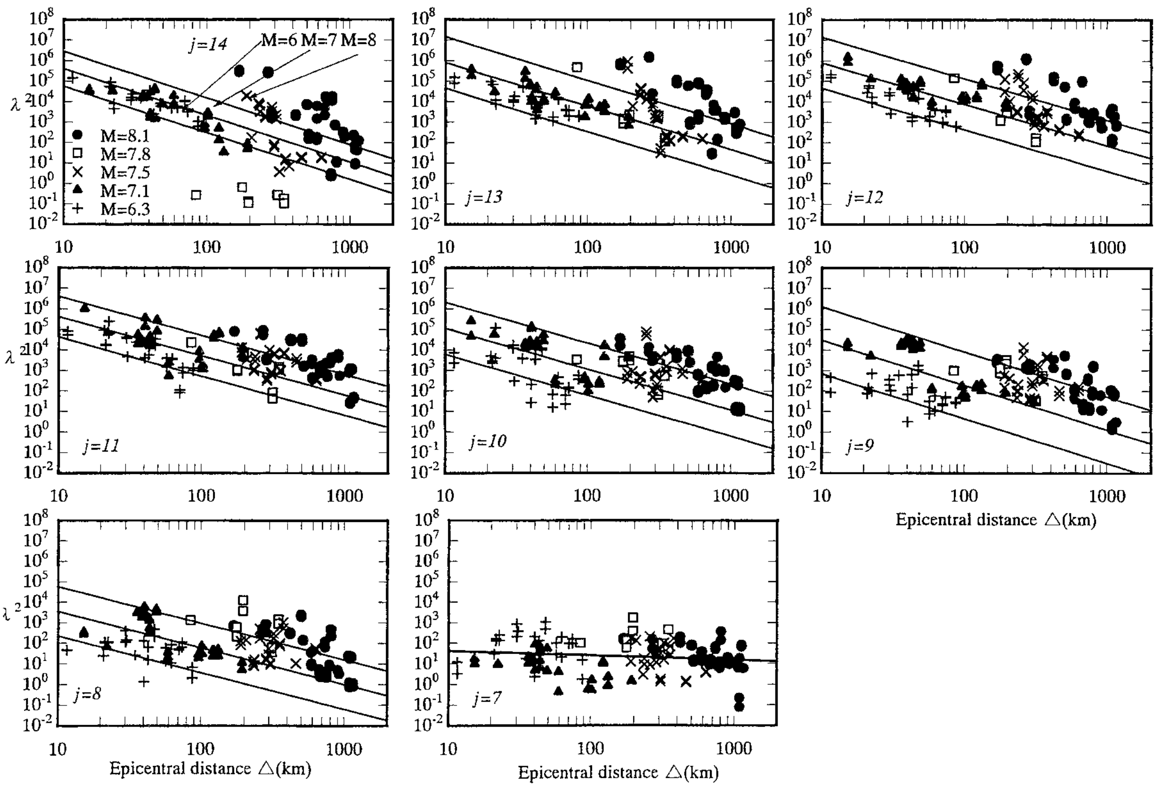

Fig. 10 Attenuation relationships for the power of earthquake motion on the jth compact support

Table 1 Regression analyses results

j	$\alpha_1^{(j)}$	$\alpha_2^{(j)}$	$\alpha_3^{(j)}$	$\beta_1^{(j)}$	$\beta_2^{(j)}$	$\beta_3^{(j)}$	$\gamma_1^{(j)}$	$\gamma_2^{(j)}$	$\gamma_3^{(j)}$	the correlation coefficients		
										$\mu_{tgr}^{(j)}$	$\sigma_{tgr}^{(j)}$	$\lambda^{(j)}$
7	1.011	27.71	5.26E+1	0.0	0.0	0.0185	0.864	0.203	-0.219	0.86	0.41	0.14
8	0.830	14.58	8.53e-4	0.049	0.0	1.200	0.790	0.337	-1.779	0.94	0.71	0.59
9	0.543	17.97	1.90e-5	0.096	-0.030	1.626	0.700	0.344	-2.187	0.85	0.75	0.68
10	0.806	8.45	1.41e-2	0.060	-0.005	1.270	0.686	0.321	-1.990	0.97	0.73	0.64
11	0.850	2.97	3.78e+0	0.026	0.016	0.993	0.764	0.366	-1.908	0.98	0.77	0.69
12	0.511	0.39	1.66e-1	0.058	0.143	1.244	0.744	0.295	-2.023	0.99	0.83	0.69
13	0.367	0.08	1.76e-1	0.077	0.267	1.254	0.739	0.201	-2.117	0.99	0.87	0.65
14	0.330	0.06	8.77e+1	0.081	0.287	0.850	0.742	0.239	-2.280	0.99	0.81	0.68

5. SIMULATION OF EARTHQUAKE MOTIONS FROM SIMULATED PHASE SPECTRA

Phase spectra of earthquake motions can be simulated by the regression equations given in section 4. Appling the method developed in section 3, earthquake motions compatible with the phase spectra can be simulated as follows:

(1) Procedure

The proposed simulation method is composed of next nine steps.

(i) Decide an earthquake magnitude M and an epicentral distance Δ.

(ii) Calculate $\mu_{tgr}^{j}(\omega)$ and $\sigma_{tgr}^{j}(\omega)$ using the regression equations.

(iii) Generate random numbers based on normal distribution $N(\mu_{tgr}^{j}, \sigma_{tgr}^{j})$ then calculate $t_{gr}^{j}(\omega)$. Obtain a phase spectrum $\phi_j(\omega)$ by integrating this value with respect to ω.

(iv) Simulate a time history $f_j'(t)$ on the jth scale factor using a simulated phase spectrum $\phi_j(\omega)$ and amplitude spectrum $F_j'(\omega)$ with the value of 1.0 within the frequency range $\{f \mid 2^{j-1}/T \leqq f \leqq 2^j/T\}$ and 0.0 outside of that range.

(v) Take Fourier transform on $f_j'(t)$ and obtain a new phase spectrum $\phi_j'(\omega)$

(vi) Calculate relative values of wavelet coefficient $\bar{a}_{jk}$. using this phase spectrum $\phi_j'(\omega)$.

(vii) Calculate a_{j0} from the regression equation of power λ_j^2 and obtain wavelet coefficient a_{jk} by multiplying a_{j0} by $\bar{a}_{jk}$.

(viii) Obtain a time history $f_j(t)$ on the jth scale factor using the inverse wavelet transformation.

(ix) Summing up $f_j(t)$ for a certain range of j values give the artificial earthquake motion.

The wavelet coefficient a_{jk} can be obtained directly form the phase spectrum on the jth scale factor by the method developed in section 2. Steps (iv) and (v) seem redundant, but without them a time history, $f_j(t)$ can not be properly simulated. The phase spectrum and Fourier amplitude of $f_j(t)$ overlap the neighboring scale factors in the frequency ranges $\{2^j/3T<f<2^{j-1}/T\}$ and $\{2^j/T<f<2^{j+1}/3T\}$. This effect is avoided by assigning 0.0 to the Fourier amplitude within these frequency ranges in steps (iv) and (v).

(2) Examples of simulated earthquake motions

Earthquake motions of magnitude M=8 are simulated for three epicentral distances: 50(km), 100(km) and 200(km). Because a set of random values is used to simulate group delay time on the scale factors, concerned the simulated earthquake motion is a sample from the mother set of time histories. Examples of simulated results are shown in Figs.11 and 12. Time histories for several scale factors that cover important frequency ranges for the seismic design of civil structures are shown in Fig.11. Artificial earthquake motions obtained by summing up all the time histories related to the scale factors concerned are shown in Fig.12.

Fig.11 shows that the main arrival time of the time history delays as a scale factor decreases as the epicentral distance increases. Fig.12 shows a decrease in maximum acceleration and elongation of duration as the epicentral distance increases and that longer period motion predominates in the later part of simulated earthquake motions, especially for a long epicentral distance.

(3) Verification of simulated earthquake motions

Values of the maximum accelerations and velocities obtained from simulated earthquake motions were compared with an existing attenuation relationship of maximum acceleration and velocity to show the efficiency of the proposed simulation method. Several attenuation relationships are proposed based on the concept of equivalent source distance (Ohno et al. 1993) and shortest distance to the earthquake fault (Fukushima 1994). But the attenuation relationship used here is the simple one proposed by Kawashima et al. (1984) because the earthquake magnitude M and epicentral distance Δ were selected as parameters of the regression relationship of group delay time. Results are shown in Fig.13 in which data obtained for M=8.0 with is plotted for epicentral distances of 50, 100 and 200 km. Several data points are at the same epicentral distance because the sample earthquake motions could be simulated from different sets of random values. Simulated maximum accelerations have small values for long epicentral distances when compared with Kawashima's attenuation relationship but the maximum velocities fit the attenuation relationship well. In our regression relationship there is no term to account for the saturation effect in the near source region; therefore, the estimation of large maximum accelerations and velocities in the near source region is possible.

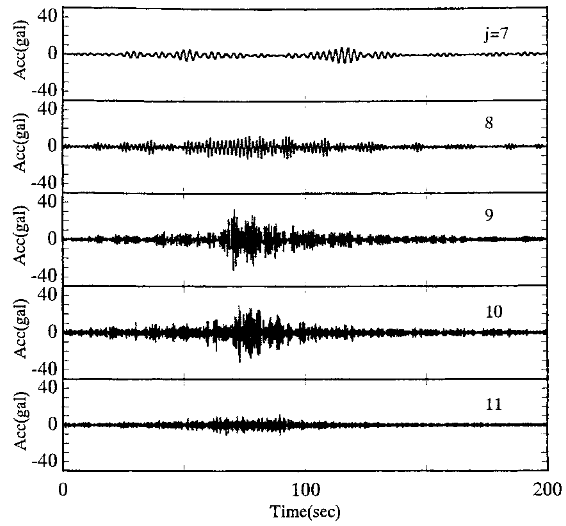

(a) M=8, △=200(km)

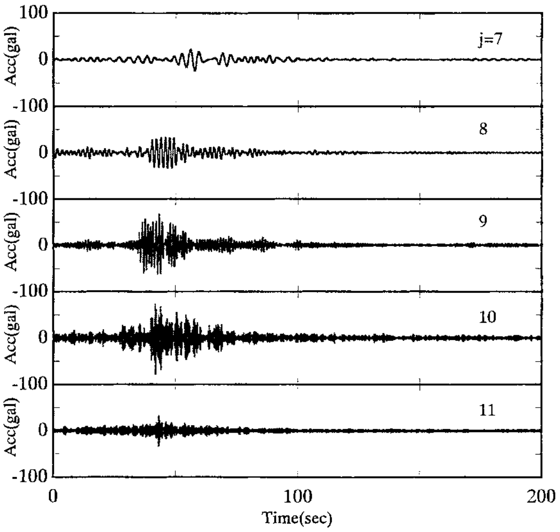

(b) M=8, △=100(km)

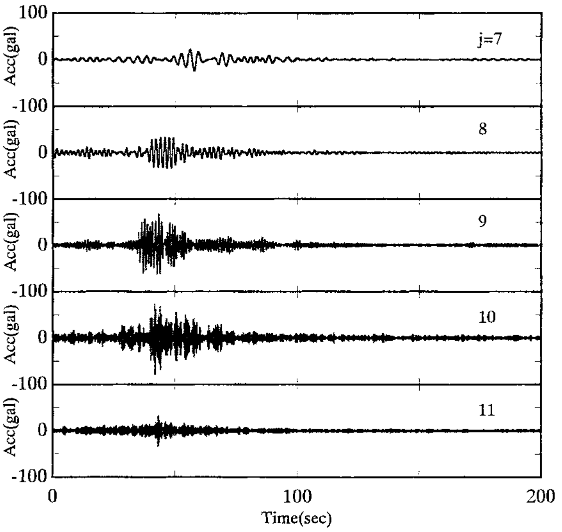

(b) M=8, △=100(km)

Fig. 11 Simulated wave for scale factors j=7−11 based on attenuation relationships (M=8)

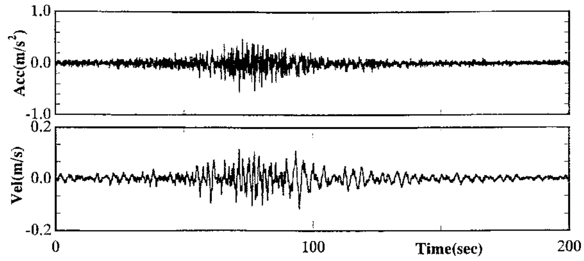

(a) M8, △=200(km)

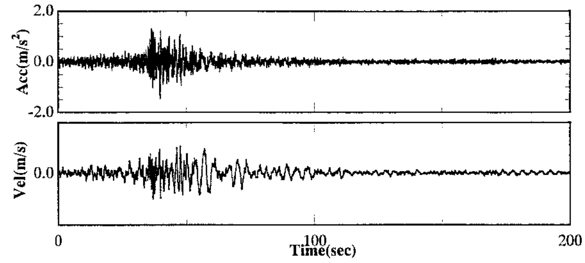

(b) M8, △=100(km)

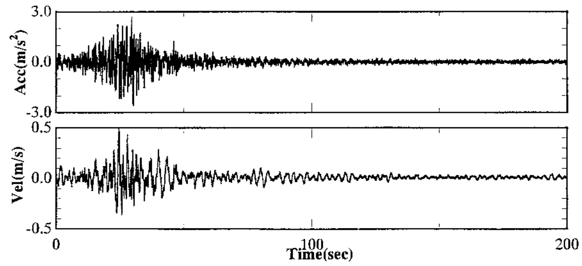

(c) M8, △=50(km)

Fig. 12 Simulated seismograms for M=8, Δ=50, 100 and 200 (km)

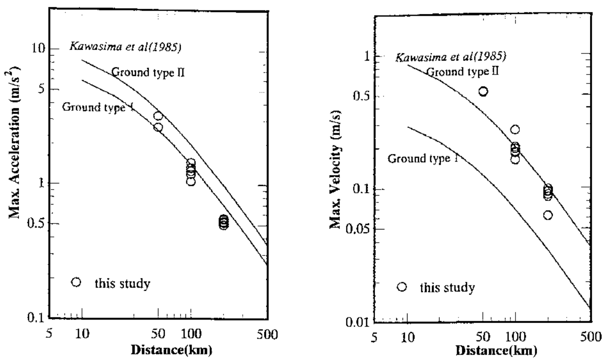

Fig. 13 Maximum acceleration and velocity values of simulated waves as comparedwith M-Δ relation (Kawashima *et al*)

6. CONCLUSION

Using the wavelet transformation technique we developed a method with which to simulate earthquake motions compatible with given phase spectra. The following results were obtained.

(1) Because, using Mayer's analyzing wavelet, a decomposed time history is defined on a compact support in the frequency domain (the amplitude spectrum of the decom-

posed time history has values in a certain frequency range), the relative values of the wavelet coefficients could be obtained from the phase spectrum of this compact support.

(2) If the power of the decomposed time history on a compact support is given, the absolute values of the wavelet coefficients on this support can be calculated. Therefore the original time history was shown to be recomposed based on the inverse wavelet transform.

(3) The efficiency of simulating earthquake motion by the proposed method was evaluated by resimulating the observed earthquake motion recorded during the 1995 Far-off Sanriku earthquake.

(4) A method to simulate phase spectra that uses the concept of group delay time was introduced, as were the regression relationships of the mean value and standard deviation of the group delay time on the compact support as functions of earthquake magnitude and epicentral distance. The regression relationship of the power of earthquake motion on the compact support was derived.

(5) A phase spectrum was obtained by integrating the simulated group delay time using proposed regression relationship. Earthquake motion compatible with the phase spectrum then was simulated.

(6) The appropriateness of the earthquake motions simulated by our novel method to for seismic design purpose was verified by a comparison with existing attenuation characteristics of maximum acceleration and velocity

REFERENCES

Arakawa, T., Kawashima, K. and Aizawa, K. (1984). “Input ground motions for step-by-step integration dynamic response analysis by modifying response spectral characteristics”, *Civil Engineering Journal*, Vol.26, No.7 (in Japanese).

Fukushima,Y. (1994), “Empirical prediction for strong ground motion reflected on theoretical backgrounds of source and propagation of seismic wave”, *ORI Report* 93-07, Ohsaki Research Institute, (in Japanese).

Goto, H., Kameda, H. and Sugito, M. (1979), “Prediction of strong earthquake motions by the evolutionary precess model”, *J. Struct. Mech. Earthquake Eng.*, JSCE, No.286, 37-51 (in Japanese).

Irikura, K. (2000), “Prediction of strong motions from future earthquakes caused by active faults: case of the Osaka basin”, *Proc. the 12th World Conference on Earthquake Engineering*, Paper No.2687.

Ishii, T. and Watanabe, T. (1987). “Relation between phase characteristics of ground motions and magnitudes, focal distances and focal depths of earthquakes”, *Summaries of Technical Papers of Annual Meetings of AIJ, Structures I*, 385-386 (in Japanese).

Izumi, M. and Katukura, H. (1980). "Representation of nonstationary nature of seismic waves based on phase (Part I)”, *Proc. of the International Research Conference on Earthquake Engineering*,199-212.

Japan Society Civil Enginners (1996), “Proposal on earthquake resistance for civil engineering structures”, Special report of the committee of earthquake resistance on civil engineering structures, Japan.

Jennings, P. C., Housner, G. W. and Tstai, N. C. (1968). “Simulated earthquake motions for design purposes”, *Proc. of the 4-th World Conference on Earthquake Engineering,* A-1, 145-160.

Joyner, W. B. and Boore, D. M. (1981): “Peak horizontal acceleration and velocity from strong-motion records, including records from 1979 Imperial Valley, California, earthquake”, *Bulletin of Seismological Society of America*, 71, 2011-2038.

Kameda, H. (1977), “On a method of computing evolutionary power spectra of strong motion seismograms”, *J. Struct. Mech. Earthquake Eng., JSCE*, No.235, 55-62 (in Japanese).

Kamiyama, M. and Yanagisawa, E. (1986), “A statistical model for estimating response spectra of strong earthquake motions with emphasis on local soil conditions”, *Soil and Foundations*, 26, 16-32.

Kawashima, K., Aizawa, K. and Takahashi, K. (1984), “Attenuation of peak ground motions and absolute acceleration response spectra”, *Proc. the 8th World Conference on Earthquake Engineering*, 257-264.

Meyer, Y. (1989), “Orthonormal wavelets in wavelets”, Springer, 21-27.

Ohno, S., Ohta, T. Ikeura, T. and Takemura M. (1993), “Revision of attenuation formula considering the effects of fault size to evaluate strong motion spectra in the near field”, *Tectonophysics*, 218, 69-81.

Ohno, S., Takemura, M. and Kobayashi, Y. (1998), “Near-fault rupture directivity effects on strong-motion records”, *Proc. of the 10th Japan Earthquake Engineering Symposium*, 133-138 (in Japanese).

Ohsaki, Y., Kanda, J., Iwasaki, R., Masao, T., Kitasa, T. and Sakata, K. (1984). “Improved methods for generation of simulated earthquake ground motions”, *Proc. the 8th World Conference on Earthquake Engineering*, 573-580.

Sasaki, F., Maeda, T. and Yamada, M. (1992). “Study of time history data using the wavelet transform”, *J. Struc. Eng., AIJ*, Vol.38BÅC9-20 (in Japanese).

Sato, T., Murono, Y. and Nishimura A. (1999a). “Modeling of phase characteristics of strong earthquake motion”, *J. Struct. Mech. Earthquake Eng., JSCE*, No.612/I-46, 201-213 (in Japanese).

Sato, T., Murono, Y. and Nishimura A. (1999b). “Modeling of phase spectrum to simulate design earthquake motion”, *Optimizing post-earthquake lifeline system reliability, Technical Council on Lifeline Earthquake Engineering*, Monograph No.16, 804-813.

Satoh, T., Uetake, T. and Sugawara, Y. (1996). “A study on envelope characteristics of strong motions in a period range of 1 to 15 seconds by using group delay time”, *Proc. of 11th World Conference on Earthquake Engineering*, Paper No.149.

Sawada, T., Nagae, M. and Hirao, K. (1986), “A definition of the duration of earthquake ground motion based on phase differences and its statistical analysis”, *J. Struct. Mech. Earthquake Eng., JSCE*, No.368/I-5, 373-382 (in Japanese).

Trifunac, M. D. (1976). “Preliminary empirical model for scaling Fourier amplitude spectra of strong ground accleration in terms of earthquake magnitude, source-to-station distance, and recording site conditions”, *Bulletin of Sesimological Soc. of Am.*, Vol.66, No.4, 1343-1373.

Yang, J. N. (1972), “Simulation of random envelope process”, *Journal of Sound and Vibration*, Vol.21, No.73.